Ilmenau Package for Model Order Selection and Evaluation of Model Order Estimation Scheme of Users of MIMO Channel Sounders

João Paulo C. Lustosa da Costa[1], Florian Roemer[2], Flávio A. de Castro Jr.[1],
Rafael F. Ramos[1], Lola Sabirova[1], and Stefanie Schwarz[1,3]

***Resumo*— Em vários campos da ciência, a análise de componentes principais (PCA) é aplicada para extrair informação de dados e um primeiro passo crucial para a PCA é a estimação da quantidade de componentes principais, também conhecida como ordem do modelo. Por exemplo, em processamento de sinais em arranjos de sensores, técnicas robustas para estimação da ordem do modelo são necessárias, já que na prática somente uma quantidade limitada de observações está disponível.**

Neste artigo, nós propomos um programa chamado Ilmenau package para seleção da ordem do modelo (IPM) a fim de comparar diversas técnicas de seleção de ordem do modelo estado da arte. Nós mostramos que uma técnica de estimação de ordem do modelo pode superar outra técnica para um certo cenário e por isso é importante que se tenha um programa que avalie qual é a melhor técnica para um cenário desejado. Outra contribuição importante deste artigo é comparar o desempenho da técnica de estimação de ordem do modelo de usuários da sonda de canais MIMO com as técnicas de seleção de ordem de modelo que são estado da arte.

***Palavras-Chave*— Seleção da ordem do modelo, análise de componentes principais.**

***Abstract*— In several scientific fields, principal component analysis (PCA) is applied to extract information from the data and the first crucial step for PCA is the estimation of the amount of principal components, also known as model order. For instance, for sensor array signal processing, robust techniques for the estimation of the model order are needed, since in practice only a limited number of observations is available.**

In this paper, we propose a software called Ilmenau package for model order selection (IPM) to compare the several state-of-the-art model order selection schemes in the literature. Since one model order estimation scheme can outperform another scheme for only a certain scenario, it is important to have such a software that evaluates which scheme is the best for a desired scenario. Another major contribution of this paper is to compare the performance of the model order estimation scheme of users of MIMO channel sounders to the state-of-the-art model order selection schemes.

***Keywords*— Model Order Selection, Principal Component Analysis.**

I. Introduction

There are several state-of-the-art model order selection (MOS) schemes in the literature and the performance of each MOS scheme depends on the scenario parameters such as the array size, the number of snapshots, the level of noise correlation and the level of the signals correlation. Therefore, it is not possible to affirm, based on the literature, which of the state-of-the-art MOS technique achieves the Probability of correct Detection (PoD) for different scenarios.

In order to help in the choice of the best model order selection scheme for a certain desired scenario, we propose the Ilmenau Package for Model Order Selection (IPM)[1], and it is a software that allows to compare several state-of-the-art model order selection scheme for a desired scenario. With IPM, the user can choose the best scheme for his specific scenario. In addition, we show that by assuming a data model with centro-symmetric arrays, the model order estimation of most schemes is improved via forward backward averaging (FBA) [1], [2].

Additionally, we present a matrix-based model order selection technique based on ESPRIT [3], whose the main algorithm is similar to the one used by users of MIMO channel sounders (UMCS) [4]. Limitations of this practical MOS approach are shown, as well as simulations comparing it to other matrix-based MOS schemes.

The remainder of this paper is organized as follows. First we review the tensor and matrix notation in Section II and we present the data model in Section III. Then the UMCS scheme for model order selection is formely presented in Section IV, while the Ilmenau Package for Model Order Selection is proposed in Section V. The simulations results are presented in Section VI and the conclusions are drawn in Section VII.

II. Tensor and matrix notation

In order to facilitate the distinction between scalars, matrices, and tensors, the following notation is used: Scalars are denoted as italic letters ($a, b, \ldots, A, B, \ldots, \alpha, \beta, \ldots$), column vectors as lower-case bold-face letters ($\boldsymbol{a}, \boldsymbol{b}, \ldots$), matrices as bold-face capitals ($\boldsymbol{A}, \boldsymbol{B}, \ldots$), and tensors are written as bold-face calligraphic letters ($\boldsymbol{\mathcal{A}}, \boldsymbol{\mathcal{B}}, \ldots$). Lower-order parts are consistently named: the (i, j)-element of the matrix $\boldsymbol{A}$, is denoted as $a_{i,j}$ and the (i, j, k)-element of a third order tensor $\boldsymbol{\mathcal{X}}$ as $x_{i,j,k}$. The n-mode vectors of a tensor are obtained by varying the n-th index within its range $(1, 2, \ldots, I_n)$ and keeping all the other indices fixed.

We use the superscripts $^{\mathrm{T}}$, $^{\mathrm{H}}$, *, and $^{+}$ for transposition, Hermitian transposition, conjugate, and the Moore-Penrose

[1] Electrical Engineering Department, University of Brasília (UnB), Brazil. [2] Communications Research Laboratory, Ilmenau University of Technology, Germany. [3] Stefanie Schwarz is also a student from the Munich University of Technology and an intern of the RISE Program at UnB supported by the Deutscher Akademischer Austauschdienst (DAAD). E-mails: joaopaulo.dacosta@ene.unb.br, florian.roemer@tu-ilmenau.de.

[1]The IPM can be downloaded at http://www.pgea.unb.br/~lasp/.

pseudo inverse of matrices, respectively. The operator $\|\cdot\|_F^2$ denotes the Frobenius norm.

The n-th unfolding of $\boldsymbol{\mathcal{A}}$ is represented by $\boldsymbol{\mathcal{A}}_{(n)}$, and is the matrix form of $\boldsymbol{\mathcal{A}}$ varying the n-th index along the rows and stacking all the other indices along the columns of $\boldsymbol{\mathcal{A}}_{(n)}$.The n-mode product is defined as the product between a matrix $\boldsymbol{B}$ and $\boldsymbol{\mathcal{A}}_{(n)}$, and it is written in the following fashion $\boldsymbol{\mathcal{A}} \times_n \boldsymbol{B}$.

III. Data model

In general, the observations may be modeled as a superposition of d damped exponentials sampled on an R-dimensional grid of size $M_1 \times M_2 \times \ldots \times M_R$ at N subsequent time instants. The measurement samples are given by

$$x_{m_1,m_2,\ldots,m_R,n} = \sum_{i=1}^{d} s_i(n) \prod_{r=1}^{R} e^{(m_r-1)\cdot\left(\zeta_i^{(r)}+j\cdot\mu_i^{(r)}\right)} + n^{(c)}_{m_1,m_2,\ldots,m_R,n}, \quad (1)$$

where $m_r = 1,2,\ldots,M_r$ for $r = 1,2,\ldots,R$, $n = 1,2,\ldots,N$, $s_i(n)$ denotes the complex amplitude of the i-th exponential at time instant n, $\mu_i^{(r)}$ symbolizes the spatial frequency of the i-th exponential in the r-th mode, $\zeta_i^{(r)} \leq 0$ represents the corresponding damping factor, and $n^{(c)}_{m_1,m_2,\ldots,m_R,n}$ models the additive colored noise component inherent in the measurement process. In the context of array signal processing, each of the exponentials represents one planar wavefront and the complex amplitudes $s_i(n)$ are the symbols. It is our goal to estimate the number of impinging signals d.

In the classical matrix approach, (1) is transformed into a matrix-vector equation by defining an array steering matrix [5]

$$\boldsymbol{A} = \boldsymbol{A}^{(1)} \diamond \boldsymbol{A}^{(2)} \ldots \diamond \boldsymbol{A}^{(R)} \in \mathbb{C}^{M\times d} \quad (2)$$
$$\boldsymbol{A}^{(r)} = \left[\boldsymbol{a}^{(r)}\left(\mu_1^{(r)}\right), \boldsymbol{a}^{(r)}\left(\mu_2^{(r)}\right), \ldots, \boldsymbol{a}^{(r)}\left(\mu_d^{(r)}\right)\right],$$

where $\diamond$ is the Khatri-Rao operator, also known as column-wise Kronecker product, $M = \prod_{r=1}^{R} M_r$ and the vector $\boldsymbol{a}^{(r)}\left(\mu_i^{(r)}\right) \in \mathbb{C}^{M_r\times 1}$ denotes the array response in the r-th dimension for the i-th source. Here, all the spatial dimensions are stacked into column vectors. This stacking operation allows us to write the measurement equation in matrix form

$$\boldsymbol{X} = \boldsymbol{A}\cdot\boldsymbol{S} + \boldsymbol{N}^{(c)}, \quad (3)$$

where $\boldsymbol{X} \in \mathbb{C}^{M\times N}$ now contains the measurements stacked in a similar fashion as in $\boldsymbol{A}$, the matrix $\boldsymbol{S} \in \mathbb{C}^{d\times N}$ contains the symbols $s_i(n)$ and the noise samples are collected in the matrix $\boldsymbol{N}^{(c)} \in \mathbb{C}^{M\times N}$. It is obvious that the stacking operation does not capture the structure inherent in the lattice that is used to sample the data.

We therefore replace the measurement matrix $\boldsymbol{X}$ by a measurement tensor $\boldsymbol{\mathcal{X}} \in \mathbb{C}^{M_1\times M_2\times\ldots\times M_R\times N}$. Its elements are given by (1). Similarly to (3), $\boldsymbol{\mathcal{X}}$ can be modeled as

$$\boldsymbol{\mathcal{X}} = \boldsymbol{\mathcal{A}} \times_{R+1} \boldsymbol{S}^{\mathrm{T}} + \boldsymbol{\mathcal{N}}^{(c)}. \quad (4)$$

Here the matrix $\boldsymbol{S}$ is the same as in (3), the tensor $\boldsymbol{\mathcal{N}}^{(c)}$ contains the noise samples as defined in (1), and the tensor $\boldsymbol{\mathcal{A}} \in \mathbb{C}^{M_1\times M_2\times\ldots\times M_R\times d}$ is termed the array steering tensor. It can be computed from the array response vectors $\boldsymbol{a}^{(r)}(\mu_i^{(r)})$ through the outer product operator. Its i-th slice in the $(R+1)$-th mode is given by

$$\boldsymbol{\mathcal{A}}_{i_{R+1}=i} = \boldsymbol{a}^{(1)}\left(\mu_i^{(1)}\right) \circ \boldsymbol{a}^{(2)}\left(\mu_i^{(2)}\right) \circ \ldots \circ \boldsymbol{a}^{(R)}\left(\mu_i^{(R)}\right), \quad (5)$$

$i = 1,2,\ldots,d$. Consequently, in the absence of noise, (4) may be rewritten as

$$\boldsymbol{\mathcal{X}} = \sum_{i=1}^{d} \boldsymbol{a}^{(1)}\left(\mu_i^{(1)}\right) \circ \boldsymbol{a}^{(2)}\left(\mu_i^{(2)}\right) \circ \ldots \circ \boldsymbol{a}^{(R)}\left(\mu_i^{(R)}\right) \circ \boldsymbol{s}_i^{\mathrm{T}}, \quad (6)$$

where $\boldsymbol{s}_i^{\mathrm{T}}$ is the i-th row of $\boldsymbol{S}$. An important consequence we can draw from (6) is that, in the absence of noise, the tensor $\boldsymbol{\mathcal{X}}$ has rank d.[2] Therefore, all the n-ranks of $\boldsymbol{\mathcal{X}}$ are at most d. Note that the matrix and tensor data model are connected through the relations $\boldsymbol{A}^{\mathrm{T}} = [\boldsymbol{\mathcal{A}}]_{(R+1)}$ and $\boldsymbol{X}^{\mathrm{T}} = [\boldsymbol{\mathcal{X}}]_{(R+1)}$. As in [6], the multi-dimensional colored noise is assumed to have a Kronecker structure, which can be written as

$$\left[\boldsymbol{\mathcal{N}}^{(c)}\right]_{(R+1)} = \boldsymbol{L}_{R+1}\cdot[\boldsymbol{\mathcal{N}}]_{(R+1)}\cdot\left(\boldsymbol{L}_1 \otimes \boldsymbol{L}_2 \otimes \ldots \otimes \boldsymbol{L}_R\right)^{\mathrm{T}}, \quad (7)$$

where $\otimes$ represents the Kronecker product, $\boldsymbol{\mathcal{N}} \in \mathbb{C}^{M_1\times M_2\ldots\times N}$ is a tensor with i.i.d. Zero Mean Circularly Symmetric Gaussian (ZMCSCG) elements, and $\boldsymbol{L}_r \in \mathbb{C}^{M_r\times M_r}$ is a correlation factor of the r-th dimension of the colored noise tensor. Similarly to [6], we can rewrite (7) by using the n-mode products in the following fashion

$$\boldsymbol{\mathcal{N}}^{(c)} = \boldsymbol{\mathcal{N}} \times_1 \boldsymbol{L}_1 \times_2 \boldsymbol{L}_2 \ldots \times_R \boldsymbol{L}_R \times_{R+1} \boldsymbol{L}_{R+1}. \quad (8)$$

The noise covariance matrix in the i-th mode $\boldsymbol{W}_i$ is defined as

$$\mathrm{E}\left\{\left[\boldsymbol{\mathcal{N}}^{(c)}\right]_{(i)}\cdot\left[\boldsymbol{\mathcal{N}}^{(c)}\right]_{(i)}^{\mathrm{H}}\right\} = \alpha\cdot\boldsymbol{W}_i = \alpha\cdot\boldsymbol{L}_i\cdot\boldsymbol{L}_i^{\mathrm{H}}, \quad (9)$$

where α is a normalization constant, such that $\mathrm{tr}(\boldsymbol{L}_i\cdot\boldsymbol{L}_i^{\mathrm{H}}) = M_i$. The equivalence between (7), (8), and (9) is shown in [6].

For centro-symmetric arrays, forward-backward averaging (FBA) [1] may be incorporated as a preprocessing step. Thereby, we virtually double the number of available snapshots without sacrificing array aperture. The FBA is obtained by replacing the measurement matrix $\boldsymbol{X} \in \mathbb{C}^{M\times N}$ by a modified matrix $\boldsymbol{Z} \in \mathbb{C}^{M\times 2N}$ given by [5]

$$\boldsymbol{Z} = \left[\boldsymbol{X} \quad \boldsymbol{\Pi}_M \boldsymbol{X}^* \boldsymbol{\Pi}_N\right], \quad (10)$$

where $\boldsymbol{\Pi}_n$ represents the $n\times n$ exchange matrix having ones on its anti-diagonal and zeros elsewhere.In [2], it is demonstrated that in the tensor case, forward-backward averaging can be expressed in the following form

$$\boldsymbol{\mathcal{Z}} = \left[\boldsymbol{\mathcal{X}} \sqcup_{R+1} \boldsymbol{\mathcal{X}}^* \times_1 \boldsymbol{\Pi}_{M_1} \ldots \times_R \boldsymbol{\Pi}_{M_R} \times_{R+1} \boldsymbol{\Pi}_N\right], \quad (11)$$

where $[\boldsymbol{\mathcal{A}} \sqcup_n \boldsymbol{\mathcal{B}}]$ represents the concatenation of two tensors $\boldsymbol{\mathcal{A}}$ and $\boldsymbol{\mathcal{B}}$ along the n-th mode.

IV. Model Order Selection Scheme of Users of MIMO Channel Sounders (UMCS)

In order to estimate the model order, users of MIMO channel sounders (UMCS) apply a model order scheme based on the stability of the noise power for different time instants [4]. In this Section, we present a general insight of this

[2] The rank cannot be larger than d, but it might be smaller. This occurs only in degenerate cases which are not relevant for our discussion, e.g., two coherent sources at exactly the same position.

model order selection scheme, although we know that different implementations are possible.

The UMCS model order selection based on measured noise power is divided into two steps. In the first step, noise samples $\boldsymbol{N}'$ are collected with the absence of signal components, and the noise power $\sigma'^2 = \left\| \frac{\boldsymbol{N}' \cdot \boldsymbol{N}'^{\rm H}}{N} \right\|_{\rm F}^2$ is estimated. In the second step, the noise plus signal samples $\boldsymbol{X}$ are collected. Then, the highest power components of $\boldsymbol{X}$ are gradually removed, and the power of the remaining components $\hat{\sigma}^2$ is computed. When the condition $\hat{\sigma}^2 \leq \sigma'^2$ is satisfied, the number P of the strongest components obtained is our estimate of the model order d.

Next we summarize an algorithm describing the second step of the UMCS model order selection scheme based on measured noise power, and our candidate value for the model order is represented by P.

1) $P = 1$;
2) Given noise plus signal samples $\boldsymbol{X}$, estimate the spatial frequencies $\hat{\mu}_i^{(r)}$ for $r = 1, \ldots, R$, and for $i = 1, \ldots, P$. In this step, any direction-of-arrival approach can be applied, e.g., MUSIC [7], ESPRIT [3], EM [8], or SAGE [9].
3) Given $\hat{\mu}_i^{(r)}$, compute $\hat{\boldsymbol{A}}$ considering the Vandermonde structure. Moreover, compute $\hat{\boldsymbol{S}}$, since $\hat{\boldsymbol{S}} = \hat{\boldsymbol{A}}^+ \cdot \boldsymbol{X}$. A particular structure of $\boldsymbol{S}$ can be taken into account in order to improve the estimation of $\hat{\boldsymbol{S}}$.
4) Given $\hat{\boldsymbol{S}}$ and $\hat{\boldsymbol{A}}$, then compute $\hat{\boldsymbol{X}}$.
5) Given $\hat{\boldsymbol{X}}$, $\hat{\boldsymbol{N}} = \boldsymbol{X} - \hat{\boldsymbol{X}}$ is computed. Then, $\hat{\sigma}^2 = \left\| \frac{\hat{\boldsymbol{N}} \cdot \hat{\boldsymbol{N}}^{\rm H}}{N} \right\|_{\rm F}^2$ is computed.
6) If $\hat{\sigma} \leq \alpha_{\rm PW} \cdot \sigma'$ is true, then $\hat{d} = P$ and the algorithm should stop. Otherwise, increment P and return to 2).

Note that $\alpha_{\rm PW}$ is a very important design parameter in the UMCS scheme as we show in the simulations in Section VI.

V. Ilmenau Package for Model Order Selection

In this section, we propose the Ilmenau Package for Model Order Selection, a Java$^{\rm TM}$ and MATLAB$^{\rm TM}$ based software with a simple interface that allows to verify quickly, which model order selection scheme is the best for a desired scenario. Several state-of-the-art model order selection schemes are included in IPM.

In Fig. 1, we present the initial window of IPM. As the software starts, one should click on connect in order to connect to MATLAB$^{\rm TM}$. The MATLAB$^{\rm TM}$ software opens automatically and IPM connects to it. Also in Fig. 1, the user can set the type of the desired data. For instance, the data can be set according to the number of dimensions, the array size, the number of snapshots, the signal correlation level and the noise correlation level.

Once the signal and noise information is set up, the user can click on 'Selecting Methods' as shown in Fig, 2, where the model order selection schemes to be compared are chosen. In IPM, we consider the following state-of-the-art model order selection techniques: Akaike's information theoretic criterion (AIC) [10], [11], the Minimum Description Length (MDL) criterion [10], [11], Efficient Detection Criterion (EDC) [12],

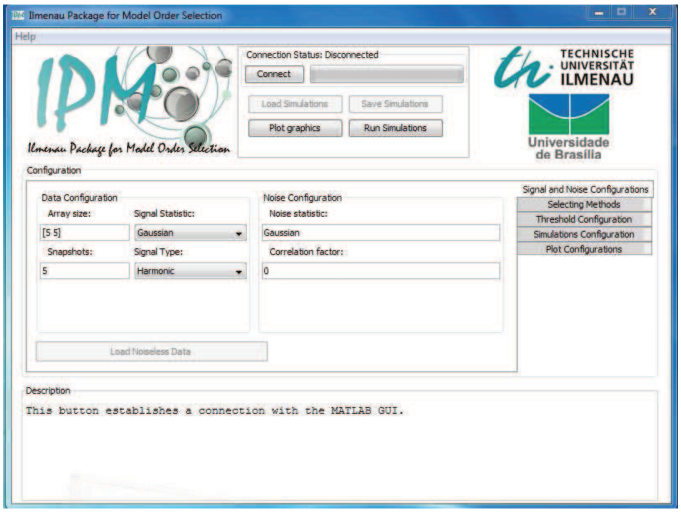

Fig. 1. IPM window with signal and noise configuration

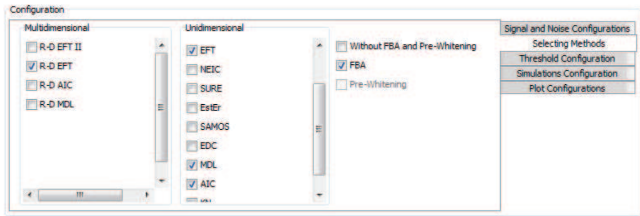

Fig. 2. IPM window to select the multi-dimensional and one dimensional model order selection schemes

[11], ESTER [13], SAMOS [14], RADOI [15], KN[3], M-EFT [16], [17], [11], EFT [18], SURE [19], and NEMO [20].

For the EFT based schemes, i.e. R-D EFT II, R-D EFT, M-EFT, and EFT, the user has to compute the threshold coefficients. It is possible to set up the threshold by clicking on 'Threshold Configuration'. Without the threshold coefficients, the EFT based schemes cannot be applied.

In Fig.4, the user can set up the simulations by clicking on 'Simulations Configuration'. Since a model order scheme can outperform another one for only a certain number of sources, the user can choose a certain interval of number of sources. The Signal to Noise Ratio (SNR) can be defined as well as the number of points to plot the curve of Probability of correct Detection (PoD) versus SNR.

Once the whole scenario is set up and the MOS schemes are chosen, the user can click on 'Run simulations'. When the simulations iterations are complete, the performance of the model order schemes for the specific scenario is shown by clicking on 'Plot graphics'.

VI. Simulation Results

In this section, we generate our samples based on the data model of (4), where the spatial frequencies $\mu_i^{(r)}$ are drawn from an uniform distribution in $[-\pi, \pi]$. The source symbols are i.i.d. ZMCSCG distributed with power equal to σ_s^2 for

[3]The KN model order selection program can be download at http://www.wisdom.weizmann.ac.il/~nadler/.

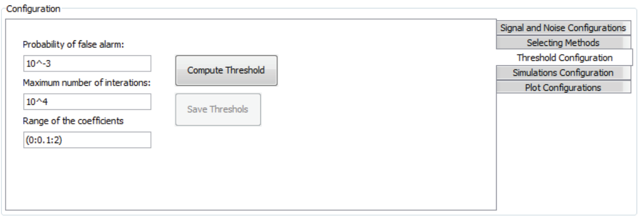

Fig. 3. IPM window to set up the threshold

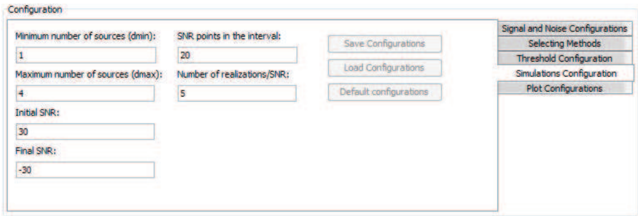

Fig. 4. IPM window for simulation configuration

all the sources. The SNR at the receiver is defined as SNR $= 10\log_{10}\left(\frac{\sigma_s^2}{\sigma_n^2}\right)$, where σ_n^2 is the variance of the elements of the white noise tensor $\boldsymbol{\mathcal{N}}$ in (7).

Here we consider that the elements of the signal covariance matrix $\boldsymbol{R}_{ss} = \mathrm{E}\{\boldsymbol{S}\boldsymbol{S}^{\mathrm{H}}\} \in \mathbb{C}^{d\times d}$ vary as a function of the correlation coefficient ρ_s. As an example we consider in (12) the structure of $\boldsymbol{R}_{ss}$ as a function of ρ_s for $d = 3$

$$\boldsymbol{R}_{ss} = \begin{bmatrix} 1 & \rho_s^* & (\rho_s^*)^2 \\ \rho_s & 1 & \rho_s^* \\ \rho_s^2 & \rho_s & 1 \end{bmatrix}, \qquad (12)$$

where ρ_s is the correlation coefficient. Note that also other types of correlation models can be used.

The Probability of correct Detection (PoD) is used to compare the performance of the several model order selection schemes. Therefore, we define the PoD as the number of realizations with correct estimated model order divided by the total number of realizations.

In Fig. 5, UMCS stands for users of MIMO channel sounders scheme. The suffix Low, Med and Hi indicates the respective variations of the design parameter $\alpha_{\mathrm{PW}} = 1$, $\alpha_{\mathrm{PW}} = 1.5$, and $\alpha_{\mathrm{PW}} = 2$, where α_{PW} is also defined in Section IV. Moreover, the suffix Mag and Vand denotes that information about $\boldsymbol{S}$ is applied to improve the estimation. Mag means that the magnitude of the elements of $\boldsymbol{S}$ should be equal to one, while Vand means that $\boldsymbol{S}$ has a Vandermonde structure.

Comparing all the curves in Fig. 5, the two with highest Probability of correct Detection (PoD) are UMCS Med and UMCS Mag Med. In general, for $\alpha_{\mathrm{PW}} = 1$, and for $\alpha_{\mathrm{PW}} = 2$, a degraded performance is obtained. For instance, in Fig. 5 for SNR = 50 dB, UMCS Med with $\alpha_{\mathrm{PW}} = 1.5$ has a PoD = 0.98, while UMCS Hi with $\alpha_{\mathrm{PW}} = 2$ has a PoD = 0, and UMCS Low with $\alpha_{\mathrm{PW}} = 1$ has a PoD = 0.75. Therefore, small variations in α_{PW} imply a severe degradation of the PoD. Hence, one first disadvantage of UMCS scheme is the instability due to α_{PW}. Note that practitioners usually set $\alpha_{\mathrm{PW}} = 1$, which in this example would give a considerable degradation in the model order estimation.

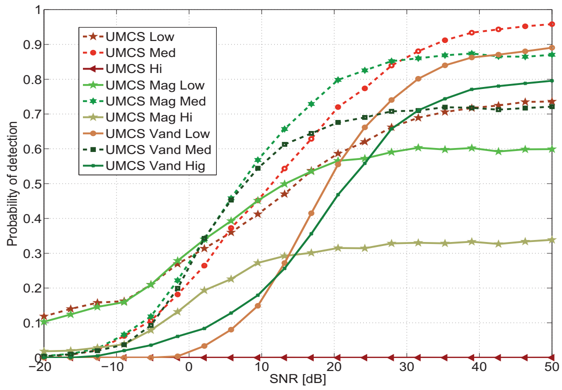

Fig. 5. Probability of correct Detection vs. SNR for an array of size $M_1 = 10$. The number of snapshots N is set to 20 and the number of sources $d = 3$.

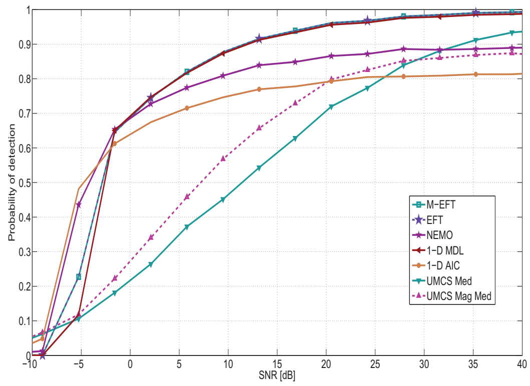

Fig. 6. Probability of correct Detection vs. SNR for an array of size $M_1 = 10$. The number of snapshots N is set to 20 and the number of sources $d = 3$.

In Fig. 6, we select the two best curves of Fig. 5 to compare to the best state-of-the-art model order selection schemes. In general, the two selected UMCS approaches are not comparable to the M-EFT, EFT, and 1-D MDL. However, they are comparable in this scenario to the 1-D AIC and the NEMO.

Note that α_{PW} is a parameter that depends on how stable the noise power is in time. If the noise power from the fist step to the second step varies 50 %, according to Fig. 5, the model order estimation is drastically degraded. Hence, UMCS scheme is very instable. Moreover, since in the best choice of α_{PW}, the PoD with UMCS scheme is close to the model order selection techniques found in the literature, it is certainly a much better option to use any state-of-the-art matrix-based model order selection present in the literature than using UMCS scheme.

In Figs. 7 and 8, we depict the PoD versus the ρ_s for $\rho_s = 0, \ldots, 0.999$. In Fig. 7, the model order selection schemes are applying without FBA, while in Fig. 8 FBA is applied. By applying FBA, an improved gain is obtained in all techniques, except for the EFT. We consider here that the signal components are correlated according to the model in (12) and ρ_s denotes the level of correlation of the signal components.

In Fig. 7, where no FBA is applied, EFT and M-EFT achieve the highest probability of detection for low signal correla-

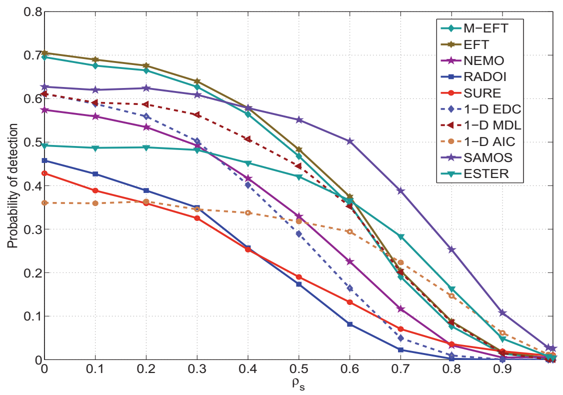

Fig. 7. PoD versus ρ_s for different model order selection schemes. Here we consider an array of size $M = 10$ with $N = 12$ snapshots. We fix the number of sources $d = 3$.

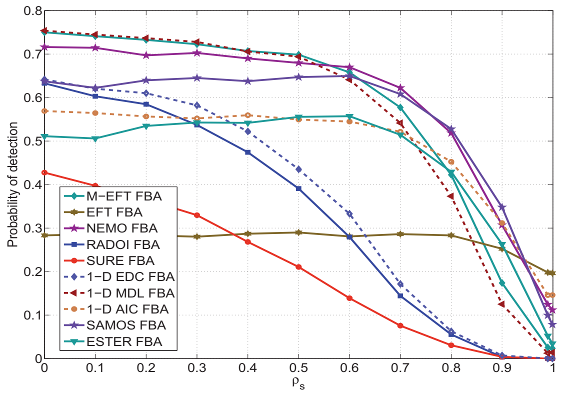

Fig. 8. PoD versus ρ_s for different model order selection schemes. Here we consider an array of size $M = 10$ with $N = 12$ snapshots. We fix the number of sources $d = 3$.

tion regimes. However, for high signal correlation regimes, SAMOS outperforms all the other schemes. In Fig. 8, where FBA is applied for all schemes, M-EFT and MDL achieve the highest probability of correct detection for low signal correlation regimes, and for high signal correlation regimes, the NEMO and SAMOS outperform the other schemes.

VII. Conclusions

In this paper, we propose the Ilmenau Package for Model Order Selection (IPM), which is a tool to compare several state-of-the-art model order selection schemes for different scenarios. As shown in simulations, there is no model order selection scheme, which is the best for all scenarios. Therefore, it is important to specify the scenario and to check with IPM, which model order selection scheme has the highest probability of correct detection (PoD).

Moreover, we show that the UMCS scheme, besides being a very unstable technique, has in the best case a probability of correct detection worse than the other model order selection schemes in the literature.

Acknowlegdments

The authors gratefully acknowledge the support of the DPP/UnB according to the announcement 03/2011 requested in UnBDoc 76780/2011.

References

[1] G. Xu, R. H. Roy, and T. Kailath, "Detection of number of sources via exploitation of centro-symmetry property," *IEEE Trans. Signal Processing*, vol. 42, pp. 102–112, Jan. 1994.

[2] F. Roemer, M. Haardt, and G. Del Galdo, "Higher order SVD based subspace estimation to improve multi-dimensional parameter estimation algorithms," in *Proc. 40th Asilomar Conf. on Signals, Systems, and Computers*, Nov. 2006, pp. 961–965.

[3] R. Roy and T. Kailath, "ESPRIT - Estimation of signal parameter via rotational invariance techniques," *IEEE Transactions on Acoustics, Speech, and Signal Processing*, vol. 37, pp. 984–995, Jul. 1989.

[4] C. B. Ribeiro, *Propagation parameter estimation in MIMO systems*. Helsinki, Finnland: Ph.D. Dissertation, Helsinki University of Technology, Apr 2008.

[5] M. Haardt and J. A. Nossek, "Simultaneous Schur decomposition of several non-symmetric matrices to achieve automatic pairing in multidimensional harmonic retrieval problems," *IEEE Trans. Signal Processing*, vol. 46, pp. 161–169, Jan. 1998.

[6] J. P. C. L. da Costa, F. Roemer, and M. Haardt, "Sequential GSVD based prewhitening for multidimensional HOSVD based subspace estimation," in *Proc. ITG Workshop on Smart Antennas*, Berlin, Germany, Feb. 2009.

[7] R. O. Schmidt, "Multiple emitter location and signal parameter estimation," *IEEE Transactions on Antennas and Propagation*, pp. 276–280, Mar. 1986.

[8] M. I. Miller and D. R. Fuhrmann, "Maximun likelihood narrow-band direction finding and the EM algorithm," *IEEE Transactions on Acoustics, Speech and Signal Processing*, vol. 38, pp. 1560–1577, 1990.

[9] J. A. Fessler and A. O. Hero, "Space-Alternating Generalized Expectation-maximization algorithm," *IEEE Transactions on Signal Processing*, vol. 42, no. 10, pp. 1–14, 1994.

[10] M. Wax and T. Kailath, "Detection of signals by information theoretic criteria," *IEEE Trans. on Acoustics, Speech, and Signal Processing*, vol. ASSP-33, pp. 387–392, 1985.

[11] J. P. C. L. da Costa, A. Thakre, F. Roemer, and M. Haardt, "Comparison of model order selection techniques for high-resolution parameter estimation algorithms," in *Proc. 54th International Scientific Colloquium (IWK'09)*, Ilmenau, Germany, Oct. 2009.

[12] L. C. Zhao, P. R. Krishnaiah, and Z. D. Bai, "On detection of the number of signals in presence of white noise," *Journal of Multivariate Analysis*, vol. 20, pp. 1–25, 1986.

[13] R. Badeau, B. David, and G. Richard, "Selecting the modeling order for the ESPRIT high resolution method: an alternative approach," in *Proc. IEEE International Conference on Acoustics, Speech and Signal Processing (ICASSP 2004)*, Montreal, Canada, May 2004.

[14] J.-M. Papy, L. De Lathauwer, and S. Van Huffel, "A shift invariance-based order-selection technique for exponential data modeling," *IEEE Signal Processing Letters*, vol. 14, pp. 473–476, Jul. 2007.

[15] E. Radoi and A. Quinquis, "A new method for estimating the number of harmonic components in noise with application in high resolution radar," *EURASIP Journal on Applied Signal Processing*, pp. 1177–1188, 2004.

[16] J. P. C. L. da Costa, M. Haardt, F. Roemer, and G. Del Galdo, "Enhanced model order estimation using higher-order arrays," in *Proc. 40th Asilomar Conf. on Signals, Systems, and Computers*, Pacific Grove, CA, USA, Nov. 2007.

[17] J. P. C. L. da Costa, M. Haardt, and F. Roemer, "Robust methods based on HOSVD for estimating the model order in PARAFAC models," in *Proc. IEEE Sensor Array and Multichannel Signal Processing Workshop (SAM'08)*, Darmstadt, Germany, Jul. 2008.

[18] A. Quinlan, J. Barbot, P. Larzabal, and M. Haardt, "Model order selection for short data: An exponential fitting test (EFT)," *EURASIP Journal on Applied Signal Processing*, 2007, special Issue on Advances in Subspace-based Techniques for Signal Processing and Communications.

[19] M. O. Ulfarsson and V. Solo, "Rank selection in noisy PCA with SURE and random matrix theory," in *Proc. International Conference on Acoustics, Speech and Signal Processing (ICASSP 2008)*, Las Vegas, USA, Apr. 2008.

[20] R. R. Nadakuditi and A. Edelman, "Sample eigenvalue based detection of high-dimensional signals in white noise using relatively few samples," *IEEE Transactions of Signal Processing*, vol. 56, pp. 2625–2638, Jul. 2008.